Scripta Materialia 129 (2017) 56–60

Contents lists available at ScienceDirect

Scripta Materialia

journal homepage: www.elsevier.com/locate/scriptamat

Regular article

The ultrafast phase-change memory with high-thermal stability based on SiC-doped antimony

Tianqi Guo [a,b,*], Sannian Song [a,**], Le Li [a,b], Xinglong Ji [a,b], Chang Li [a,b], Chang Xu [b,c], Lanlan Shen [a,b], Yuan Xue [a,b], Bo Liu [a], Zhitang Song [a], Ming Qi [a], Songlin Feng [a,c]

[a] State Key Laboratory of Functional Materials for Informatics, Shanghai Institute of Microsystem and Information Technology, Chinese Academy of Sciences, Shanghai 200050, China
[b] University of the Chinese Academy of Sciences, Beijing 100049, China
[c] Shanghai Advanced Research Institute, Chinese Academy of Sciences, Shanghai 201210, China

ARTICLE INFO

Article history:
Received 28 August 2016
Received in revised form 26 October 2016
Accepted 26 October 2016
Available online xxxx

Keywords:
High speed
Good stability
SiC
Nanocomposite
Phase transformation

ABSTRACT

The contradictory between switching speed and thermal stability has long been a huge challenge for phase-change memory applications. For providing a feasible solution, the rapid-phase-transition material — pure antimony, was incorporated with silicon carbide to complement their advantages. The characterization results elucidate that dopants situated in the grain boundary inhibit the crystal growth and enhance the stability of the temperature-sensitive amorphous state. Convincingly for devices, an ultrafast speed of 7 ns, an operational voltage requirement of only 1.0 V, a high endurance of more than 200 K and a long data retention are all demonstrated to be realizable and repeatable.

1. Introduction

Along with the coming era of the Internet of Things and Big Data, Phase-Change Memory (PCM) is one of the best candidates for new class memory that is capable to store the exponential growth data. Being the most matured device of the emerging memory solutions, it combines the characteristics of high density due to excellent scalability, good reliability attributed to long life time, and high speed owing to fast crystallization mechanism [1–3]. Nevertheless, PCM is still placed on the midst of DRAM and NAND for its deficiencies on operation speed and power consumption compared to DRAM [4]. Therefore, material improvements and new cell designs have been devoted many efforts to achieve complete replacement in recent years.

As is well known, antimony is a rapid-phase-transition material with a growth-dominated crystallization mechanism. Besides, this kind of Te-free phase change material is the environmental friendly material compared with other alloys containing Te. However, it has high crystallization rates but low archival life stability [5], which is very sensitive to the factors, such as deposition rate and time, residual gas pressure, substrate temperature, etc. [6] Thus the initially deposited antimony thin film is usually the crystalline state as seen in most relevant literatures [7,8]. In view of the fact that SiC doping was previously used to enhance the thermal stability and boost the operation speed of Sb_3Te material [9]. Here it was proposed and expected to be an effective dopant to improve the high temperature stability of this single element matter.

2. Experimental

Different groups with the increased SiC content were prepared by co-sputtering method using Sb and SiC targets. The concentration of SiC in Sb was varied by changing the radio frequency sputtering power and evaluated by energy dispersive spectroscopy (EDS). Here the low, medium and high doping concentration denote the materials of $(SiC)_{3.0}Sb_{94}$, $(SiC)_{4.5}Sb_{91}$ and $(SiC)_{6.0}Sb_{88}$, respectively in the following sections. The resistance as a function of temperature was in situ measured in a homemade chamber. Then the microstructure was investigated by transmission electron microscopy (TEM) and the bonding situation was explored by X-ray photoelectron spectroscopy (XPS). Finally, T-shaped PCM cells were prepared for device testing and operating demonstration, of which have a bottom-up construction of 190 nm bottom electrodes array and 60 nm phase-change layer, as well as 10 nm TiN and 300 nm Al, serving as the adherent layer and top electrode, respectively.

* Correspondence to: T. Guo, State Key Laboratory of Functional Materials for Informatics, Shanghai Institute of Microsystem and Information Technology, Chinese Academy of Sciences, Shanghai 200050, China.
** Corresponding author.
E-mail addresses: guotq@mail.sim.ac.cn (T. Guo), songsannian@mail.sim.ac.cn (S. Song).

http://dx.doi.org/10.1016/j.scriptamat.2016.10.034
1359-6462/

3. Results and discussion

Fig. 1(a) shows the resistance evolution as a function of temperature for the deposited films. The resistance-temperature (*R-T*) curves exhibit a precipitous drop at 196.8 °C, 235.7 °C and 250.6 °C for $(SiC)_{3.0}Sb_{94}$ (LD), $(SiC)_{4.5}Sb_{91}$ (MD) and $(SiC)_{6.0}Sb_{88}$ (HD), respectively. It precisely mirrors the phase transformation from the amorphous state to the hexagonal crystalline phase. In addition, the value of high resistance state (HRS) becomes larger simultaneously with a higher doping level, which is helpful to improve the amorphous thermal stability. Generally, the pure Sb film is low resistance state (LRS) of crystallization under the same treatment conditions, while light SiC doping significantly improves the situation. More noticeably, the amorphous-state Sb films were prepared for convenient comparison by controlling deposition time at the same growth rate as shown in Fig. 1(c), indicating ultrafast amorphous-crystalline phase transition occurs at a relatively low temperature. And then the activation energy of crystallization (E_a) and the temperature for 10-year data retention ($T_{10\text{-}yr}$) can be calculated according to the Arrhenius equation,

$$t = \tau \exp\left(\frac{E_a}{k_B T}\right)$$

where t is the time to failure, τ is a proportional time constant and k_B is Boltzmann's constant. Here in Fig. 1(b), the failure time is defined as the time when the resistance decreases to a half of its initial value at the specific temperature. It is observed that the $T_{10\text{-}yr}$ of low SiC-doped Sb is 89.6 °C approaching that of $Ge_2Sb_2Te_5$ [10]. And the lifetime goes up with a higher doping concentration rooting from larger activation energy. Additionally, the calculated E_a values are in good agreement with the data determined by Kissinger's method [11],

$$\ln\left(\frac{dT/dt}{T_c^2}\right) = C + \frac{E_a}{k_B T_c}$$

where dT/dt is the heating rate, T_c is the crystallization temperature and C is a constant. There is a clear increasing trend on the absolute value of the fitting lines' slope in Fig. 1(d), i.e. E_a. So it also provides a visual contrast to the doped films on activation energy. This convincingly illustrates the argument that SiC improves the lifetime of data by enhancing the stability of pure antimony with a larger energy barrier.

The TEM bright-field images with corresponding high-resolution TEM (HRTEM) and the associated selected area electron diffraction (SAED) patterns for two different doping levels are presented in Fig. 2. All the samples were annealed at the temperature of 300 °C for 3 min. The obvious decrease on the grain size can be clearly seen from Figs. 2(a) and (d). And in Figs. 2(b) and (e), the medium SiC-doped Sb exhibits about 20 nm-scale grain size, while high SiC-doped is mostly less than 10 nm. Also from both HRTEM images, we can see that the additional Si or C atoms that situated in the grain boundary lead to the increase of local disorder degree. It has the maximum possibility to cause a striking reduction of grain size. Like Si [12], C [13] or N [14] doping, the disorder phase remarkably inhibits the grain growth and supposedly changes the crystallization mechanism through extending the incubation time of the critical nucleus's formation. Meanwhile, the larger fraction of grain boundaries in SiC-doped Sb is the main reason why the film with higher doping concentration has larger resistance that arises from the scattering effect of defects. Further in Figs. 2(c) and (f), the restrain tendency of grain growth can also be confirmed by SAED patterns. And the diffraction rings of two samples can be identified as hexagonal

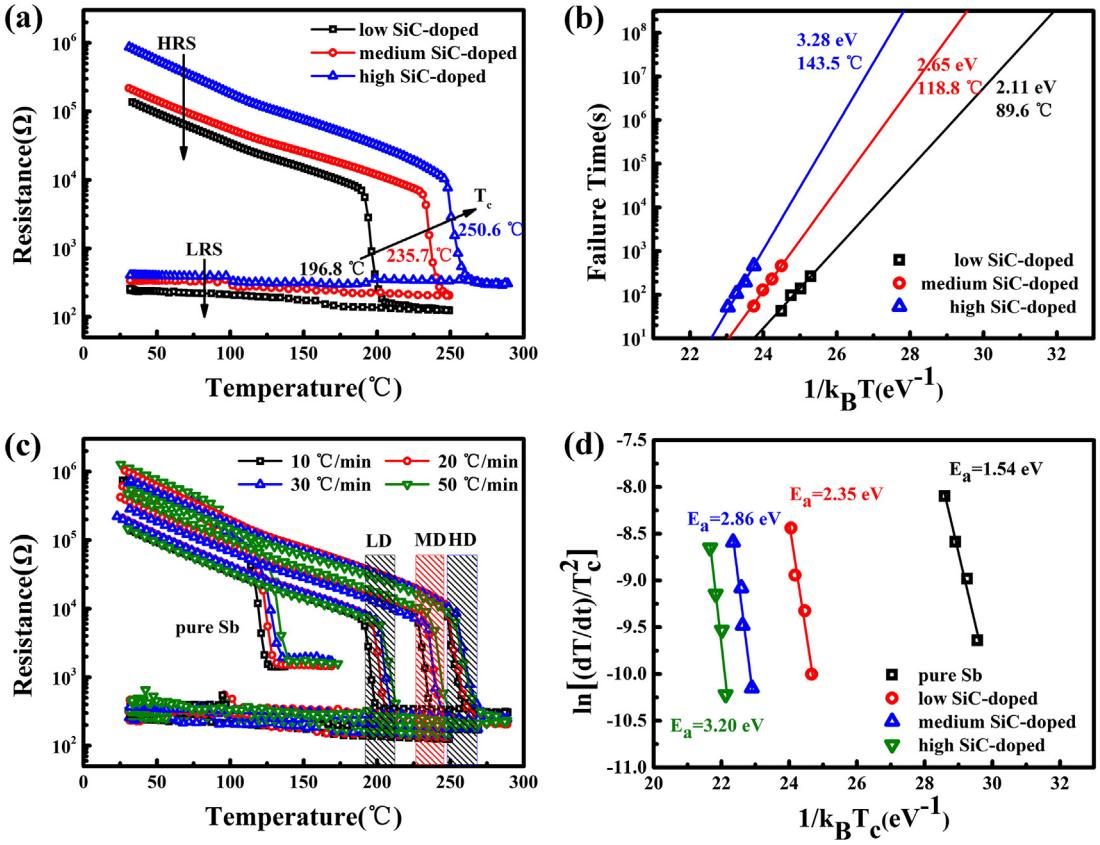

Fig. 1. (a) The resistance versus temperature measurements for as-deposited SiC-doped Sb films. The heating rate was 20 °C/min. (b) The corresponding Arrhenius extrapolation plots of failure time versus $1/k_BT$. (c) Temperature dependence of the resistance measured with various heating rates. (d) Kissinger plots for E_a calculation with regard to pure Sb and doped films.